Molecules in Environments: Toward Systematic Quantum Embedding of Electrons and Drude Oscillators

Matej Ditte[*], Matteo Barborini[†], Leonardo Medrano Sandonas, and Alexandre Tkatchenko[‡]

Department of Physics and Materials Science, University of Luxembourg, L-1511 Luxembourg City, Luxembourg

We develop a quantum embedding method that enables accurate and efficient treatment of interactions between molecules and an environment, while explicitly including many-body correlations. The molecule is composed of classical nuclei and quantum electrons, whereas the environment is modeled *via* charged quantum harmonic oscillators. We construct a general Hamiltonian and introduce a variational *Ansatz* for the correlated ground state of the fully interacting molecule-environment system. This wave function is optimized via the variational Monte Carlo method and the ground state energy is subsequently estimated through the diffusion Monte Carlo method. The proposed scheme allows an explicit many-body treatment of electrostatic, polarization, and dispersion interactions between the molecule and the environment. We study solvation energies and excitation energies of benzene derivatives, obtaining excellent agreement with explicit *ab initio* calculations and experiments.

The challenges of computational electronic-structure methods have evolved from the precise description of short-range interactions involving few electrons to the accurate modeling of longer-range many-electron effects for molecules and materials [1–3]. This shift has been enabled by the enormous progress in hardware capabilities combined with the development of new effective physical models and numerical techniques.

In particular, embedding approaches, such as the hybrid QM/MM [4–24] or QM/QM strategies [25–50], based on the partitioning of the system of interest in different subspaces, each treated with a different level of theory and thus of accuracy [1,2], have been devised to study excitation energies, solvation energies or charge transfer between fragments in a complex environment [6,11,18,24,28,38,44,51].

Even though embedding approaches can significantly improve the computational efficiency, this comes at the cost of approximating collective interactions within and between the subsystems, thus excluding important many-body effects in the overall description [1,2]. Furthermore, systems dominated by noncovalent interactions [52,53] or by static correlations [54–61] remain challenging, since they require high-level *ab initio* methods, such as coupled cluster (CC) [62] or quantum Monte Carlo (QMC) [63–65],

for which systematic convergence can be guaranteed only for relatively small systems [52,53].

In this Letter, we propose a novel approach, based on the embedding of electronic systems (atoms-molecules) within an environment of charged quantum harmonic (Drude) oscillators, which can reproduce the quantum fluctuations responsible for the noncovalent interactions and for the long-range response of realistic molecules and materials (see Fig. 1) [66–78]. Hence, our approach explicitly describes many-body correlations between the subsystem and the environment.
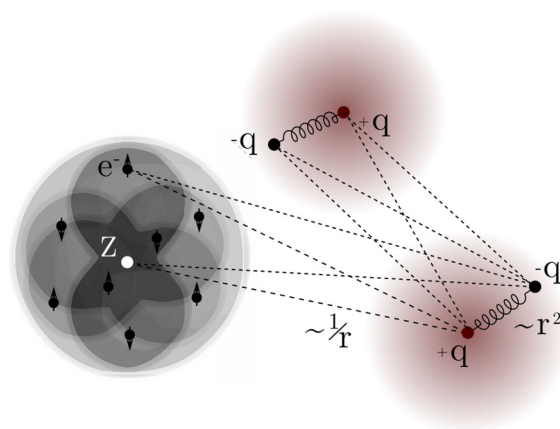

FIG. 1. Schematic representation of the embedding model for a single atom and two Drude oscillators. Strings indicate the harmonic interactions between the drudon and their corresponding centers, the dashed lines represent the Coulomb interactions between all other pairs of charged particles (for simplicity, only selected interactions are explicitly shown).

Although harmonic oscillators have been used in classical polarizable force fields [79–81], the novelty of our method lies in the quantum description of the full system of atoms and quantum Drude oscillators (QDOs) through one unified Hamiltonian for which we construct a ground state depending on all degrees of freedom. Furthermore, the proposed approach can be used with arbitrary *ab initio* methods, including CC [62] and QMC [63–65].

Within the Born-Oppenheimer approximation, each QDO consists of a pair of charged particles corresponding, respectively, to the center of the oscillator, with charge q and position $\mathbf{R}^O$ and to a distinguishable quantum particle called drudon of charge $-q$, mass μ, and position $\mathbf{r}^d$. The drudon interacts with its center via a quadratic potential $V_{\text{QDO}}(r) = \frac{1}{2}\mu\omega^2 r^2$ that depends on the mass μ and on the frequency ω that determine the slope of the quadratic well, and on their relative Euclidean distance $r = |\mathbf{r}^d - \mathbf{R}^O|$. For systems containing more QDOs, all pairs of charged particles (except the drudon and its own center) interact via the Coulomb potential. In such a model the noncovalent interactions, such as dispersion, arise from the quantum fluctuations of the charge densities that are obtained through the coupling of the quantum states of each QDO. Naturally, each QDO depends on a set of well-defined parameters $\{\mathbf{R}_i^O, q_i, \mu_i, \omega_i\}_{i=1}^{N_d}$ that are obtained by reproducing the leading order polarizabilities and dispersion coefficients of real matter [70] from accurate *ab initio* or experimental data [67,74,75,82,83].

Once the parameters have been chosen, the analytical expression of the Hamiltonian of a system of N_d interacting QDOs, the *drudonic Hamiltonian*, is written in atomic units as

$$\hat{H}^d = \sum_{i=1}^{N_d} \hat{h}_i^d(\mathbf{r}_i^d) + \sum_{i=1}^{N_d}\sum_{j>i}^{N_d} \frac{q_i q_j}{\left|\mathbf{R}_i^O - \mathbf{R}_j^O\right|} + \sum_{i=1}^{N_d}\sum_{j>i}^{N_d} \frac{q_i q_j}{\left|\mathbf{r}_i^d - \mathbf{r}_j^d\right|},$$
$$(1)$$

where $\bar{\mathbf{R}}^O = (\mathbf{R}_1^O, ..., \mathbf{R}_{N_d}^O)$ and $\bar{\mathbf{r}}^d = (\mathbf{r}_1^d, ..., \mathbf{r}_{N_d}^d)$ are the vectors of the $3N_d$ coordinates respectively of the oscillators' centers and of the drudons, and $\hat{h}_i^d(\mathbf{r}_i^d)$ are the single-body operators

$$\hat{h}_i^d(\mathbf{r}_i^d) = -\frac{1}{2\mu_i}\nabla_{\mathbf{r}_i^d}^2 + \frac{1}{2}\mu_i\omega_i^2\left|\mathbf{r}_i^d - \mathbf{R}_i^O\right|^2 - \sum_{j\neq i}^{N_d} \frac{q_i q_j}{\left|\mathbf{r}_i^d - \mathbf{R}_j^O\right|},$$
$$(2)$$

that include the kinetic energy of the *i*th drudon and its interaction energies with the oscillators' centers.

This drudonic Hamiltonian can be used to model the embedding potential that acts on a molecular system containing N_n atomic nuclei and N_e electrons, described,

respectively, by the coordinate vectors $\bar{\mathbf{R}}^n$ and $\bar{\mathbf{r}}^e$. The total Hamiltonian of electrons and QDOs (El-QDO) takes the form

$$\hat{H}^{\text{tot}} = \hat{H}^e + \hat{H}^d + \hat{V}_{\text{int}}^{d-e},$$
$$(3)$$

where $\hat{H}^e$ is the standard electronic Hamiltonian describing the interaction between the electrons and the atomic nuclei (that are parameters of the system) and $\hat{V}_{\text{int}}^{d-e}$ is the interaction between the QDOs and the atoms

$$\hat{V}_{\text{int}}^{d-e} = \sum_{i=1}^{N_e}\sum_{j=1}^{N_d} \left(\frac{q_j}{\left|\mathbf{r}_i^e - \mathbf{r}_j^d\right|} - \frac{q_j}{\left|\mathbf{r}_i^e - \mathbf{R}_j^O\right|} \right)$$
$$+ \sum_{i=1}^{N_n}\sum_{j=1}^{N_d} \left(\frac{Z_i q_j}{\left|\mathbf{R}_i^n - \mathbf{R}_j^O\right|} - \frac{Z_i q_j}{\left|\mathbf{R}_i^n - \mathbf{r}_j^d\right|} \right). \quad (4)$$

In order to describe molecular systems with static multipole moments of the charge distribution (such as the water molecule) it is necessary to introduce additional point charges in the Hamiltonian (the El-QDO Hamiltonian including the point charges is described in the Supplemental Material [84]). For example in the QDO model of water introduced by Jones *et al.* [73] and used in this work, the authors include in the model three additional point charges, centered on the two hydrogen atoms and near the oxygen atom (see Ref. [84]). These point charges do not interact with the QDOs of the corresponding molecule but only with the QDOs of the other water molecules, and in our case also with the electronic sub-system. A schematic representation of the interactions that are present in the total Hamiltonian is shown in Fig. 1. As explained below, the QDO model will be additionally corrected by an exchange-repulsion energy term that dominates the short-range interaction region [73,75,106].

The ground state of the many-body Hamiltonian defined in Eq. (3) is constructed through an appropriate variational *Ansatz* including the explicit many-body correlations between all quantum particles. In order to integrate and optimize such an *Ansatz* over the set of electronic and drudonic coordinates we choose to work in the framework of QMC methods [63,65,107], as implemented in the QMeCha package [108], although the approach can be generalized to other quantum-chemistry methods. QMC methods are stochastic integration techniques that are able of computing and minimizing the energy functional over a chosen trial wave function (see Supplemental Material [84]). In particular, we apply the variational Monte Carlo (VMC) method [63,65,107], optimizing the wave function with the stochastic reconfiguration algorithm [109,110]. Subsequently, to improve our energy estimations we use the diffusion Monte Carlo (DMC)

projection method [63,65,107] that, within the fixed-node approximation used to solve the electronic sign problem, selects the ground state component of the approximate nodal-surface given by the optimized wave function (see Supplemental Material [84]). Clearly, in the case of pure QDO systems in which the wave function is always positive and there is no nodal surface, the DMC algorithm converges to the exact solution.

We proceed to build the trial wave function for the system's ground state by expressing it as the product of three contributions

$$\Psi_{\text{tot}} = \Psi_e(\bar{\mathbf{r}}^e)\Psi_d(\bar{\mathbf{r}}^d)\mathcal{J}_{e-d}(\bar{\mathbf{r}}^e, \bar{\mathbf{r}}^d), \qquad (5)$$

which are, respectively, the electronic *Ansatz* $\Psi_e(\bar{\mathbf{r}}^e)$, the drudonic one $\Psi_d(\bar{\mathbf{r}}^d)$ and a positive-definite function $\mathcal{J}_{d-e}(\bar{\mathbf{r}}^e, \bar{\mathbf{r}}^d)$, which contains the correlation effects between the electronic and drudonic systems. In this work, the pure electronic part $\Psi_e(\bar{\mathbf{r}}^e)$ is constructed through a Slater determinant of molecular orbitals formed as linear combinations of Gaussian basis sets, multiplied by an electronic Jastrow factor used to explicitly describe the many-body correlation effects between electrons and nuclei (see Supplemental Material [84]).

The approximate form of the drudonic wave function $\Psi_d(\bar{\mathbf{r}}_d)$ is chosen to match the exact solution of a system of QDOs interacting through the dipole potential, which can be used to approximate the Coulomb potential at large distances as in the many-body dispersion MBD method [67,111]. For this reason, it is written as the exponential function of a vector-matrix-vector product

$$\Psi_d(\bar{\mathbf{r}}_d) = \exp\left[-\bar{\mathbf{r}}_{dO}^\top \mathbf{A} \bar{\mathbf{r}}_{dO}\right], \qquad (6)$$

where $\bar{\mathbf{r}}_{dO} = \bar{\mathbf{r}}^d - \bar{\mathbf{R}}^O$ is the $3N_d$ dimensional vector containing the distances between each drudon and its corresponding center, and $\mathbf{A}$ is a (symmetric) coupling matrix containing $3N_d(3N_d + 1)/2$ independent parameters. The coupling matrix explicitly correlates the drudons subject to the field of their charged centers. When this *Ansatz* is used for the Coulomb Hamiltonian in Eq. (1), multipolar contributions are captured beyond the dipole approximation.

Finally, the electron-drudon factor $\mathcal{J}_{e-d}(\bar{\mathbf{r}}^e, \bar{\mathbf{r}}^d)$ represents the coupling between the two types of quantum systems. Again, we use a vector-matrix-vector product similar to the one in Eq. (6), approximating the wave function of the electron-drudon coupling and describing the multipolar contributions arising from the full Coulomb Hamiltonian in Eq. (3)

$$\mathcal{J}_{e-d}(\bar{\mathbf{r}}^e, \bar{\mathbf{r}}^d) = \exp\left[\mathbf{d}^\top \mathbf{B} \bar{\mathbf{r}}_{dO}\right], \qquad (7)$$

coupling the distance vector $\bar{\mathbf{r}}_{dO}$ of the QDOs with the dipole moment of the molecular part

$$\mathbf{d} = \sum_{i=1}^{N_n} Z_i \mathbf{R}_i^n - \sum_{i=1}^{N_e} \mathbf{r}_i^e, \qquad (8)$$

through the rectangular matrix $\mathbf{B}$ containing a set of $3 \times 3N_d$ free parameters. We remark that the restriction of the QDO wave function to the functional form coming from the dipole approximation is not a significant limitation, since the variational optimization of the wave function parameters is followed by a DMC calculation of the many-body energy for both electrons and drudons. Being drudons distinguishable particles, DMC converges to the ground state of the QDO and El-QDO systems [112], overcoming the constraints of the *Ansätze* in Eqs. (6) and (7). An improvement of the variational *Ansatz*, without QDOs affecting the nodes of the electronic part, can only increase the efficiency of the sampling, lowering the variance of the local energy.

First, we apply our approach to Ar [113], Kr, Xe (Kr and Xe are reported in the Supplemental Material [84]) and the water dimers [114]. While these systems are small, when taken together they are challenging benchmark examples, requiring an accurate description of exchange, dispersion, polarization, and hydrogen bonding. For both Ar and water, a single QDO represents the response of all 8 valence electrons. Accordingly, the QDO model allows a significant reduction in the electronic degrees of freedom. We remark that a bosonic QDO model can be extended to describe exchange [75,115], but this would require a wave function with mixed quantum statistics for electrons and QDOs. Instead, in our current embedding scheme we describe exchange via parametrized short-range exponentials, obtained by interpolating the difference between the QDO-QDO or El-QDO PESs, and accurate CCSD(T) data [113,114]. The forms of the uncorrected PES and of the repulsive short-range functions are displayed in the Supplemental Material [84] together with their parametrization.

In Ar_2 [113], the interaction energy comes from an interplay between correlation in the long range and exchange in the short range. The attractive dispersion energy is correctly described by the QDO-QDO model and essentially coincides with its counterpart computed from electronic symmetry-adapted perturbation theory SAPT) [116] (see Supplemental Material [84]). Noticeably, the electrons-QDO (El-QDO) embedding model reproduces the full interaction curve upon subtracting the exchange contributions from SAPT, highlighting the ability of our method to capture electrostatic and polarization terms. Together with the corresponding repulsive part, both models match the reference CCSD(T) binding curve [113], as shown in Fig. 2. The same conclusions can be drawn from the dissociation curves of the Kr and Xe dimers, demonstrating the accuracy of our approach in the density overlap regime and for atoms with varying polarizability (see Supplemental Material [84]).
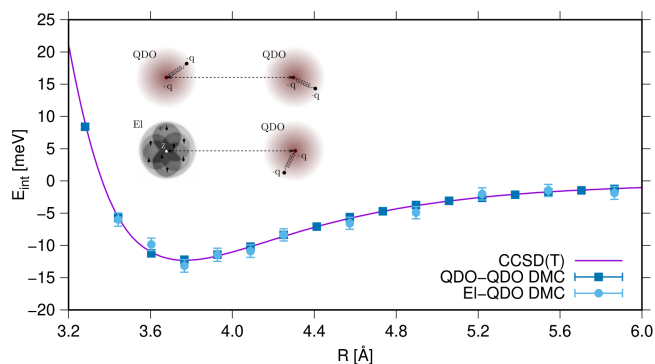
FIG. 2. Binding energy curve for the Ar dimer obtained using the QDO-QDO model and electrons-QDO (El-QDO) embedding approach (schematically shown in the figure) at the DMC level of theory, with the exponential fit of the short-range repulsion [84]. The results are compared to the CCSD(T) [113] reference curve.

For the water dimer, where intermolecular interactions are strongly directional, we apply the El-QDO embedding model to study the dissociation energies of its two lowest-energy geometric configurations, C1 and C2, along the O-O axis (Fig. 3). Here we use the extended QDO model of Martyna *et al.* [73] that contains three point charges and a QDO located at the center-of-mass, substituting the donor water molecule (on the right in Fig. 3). In this way, the lone pair of the acceptor molecule, described at the electronic level, is able to polarize during the interaction. The opposite case in which the acceptor molecule is substituted by the QDO is reported and discussed in the Supplemental Material [84]. At the equilibrium, the El-QDO method predicts comparable interaction energies in both cases, since the drudon is able to polarize towards the donor water molecules. From Fig. 3 one observes that both C1 and C2 binding curves obtained with the QDO-QDO and El-QDO models are in excellent agreement with the CCSD(T) reference [114]. The models are thus able to describe

the different interactions when varying the molecular orientation. Moreover, the comparison of the bare El-QDO interaction curve of the C1 conformer with the SAPT decomposition from Ref. [117] (see Supplemental Material [84]), shows that our model is again close to the full binding energy curve, upon subtracting the repulsive exchange contributions, thus correctly capturing both dispersion and polarization effects. From the atomic and molecular examples of Ar and water dimers, we conclude that our embedding approach is able to accurately describe the electrostatic, polarization, and dispersion interactions between an electronic subsystem and an embedding environment, in which the latter is described through a combination of QDOs and point charges.

Among the most intriguing applications of embedding approaches are the effects of solvent on the binding energies between molecules and on their electronic excitations [118,119]. Here, we study the binding in T-shaped benzene dimer, prototype for C-H $- \pi$ interactions [118,119], and the singlet-triplet excitation energy (S-T) of orthobenzyne, which is the nondiradical singlet conformer of benzyne whose excitation energy requires a proper description of dynamical correlation as well as solvent polarization [120]. These two systems are studied in cages of water from 4 to 50 molecules (see Fig. 4) with the aim of probing collective polarization and dispersion effects. In order to avoid empirical treatment of exchange in these many-body systems, we impose a minimal distance of $\sim$3 Å between the solute and water.

First we compute the solvation energies, $E_{\mathrm{Solv}}(X) = E(X_{\mathrm{Cage}}) - E(X_{\mathrm{Vacuum}}) - E_{\mathrm{Cage}}$, where X is the T-shaped benzene dimer or its monomers (Table I), in a cage composed of 50 water molecules [structures (c) and (d) in Fig. 4], or the orthobenzyne in its singlet (S) and triplet (T) spin states (Table II) in a cage of 4 and 30 water molecules [structures (a) and (b) in Fig. 4]. For all systems the El-QDO DMC results are compared
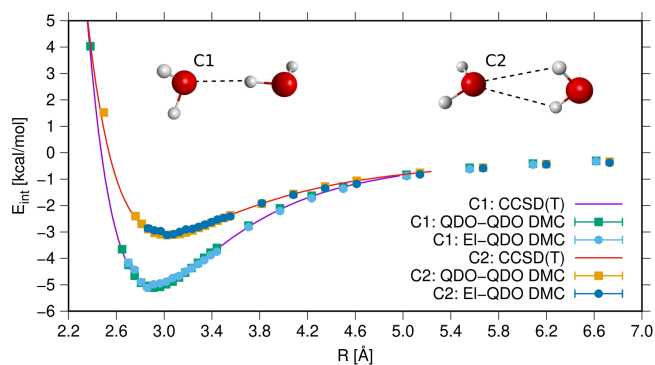

FIG. 3. Binding energy curve for the water dimer as a function of the oxygen-oxygen distance in the two energetically lowest geometric configurations (C1 and C2) [114] obtained using the QDO-QDO and El-QDO (with QDO on the right, approximating the donor) models at the DMC level of theory [84]. The results are compared to the CCSD(T) [114] reference curve.
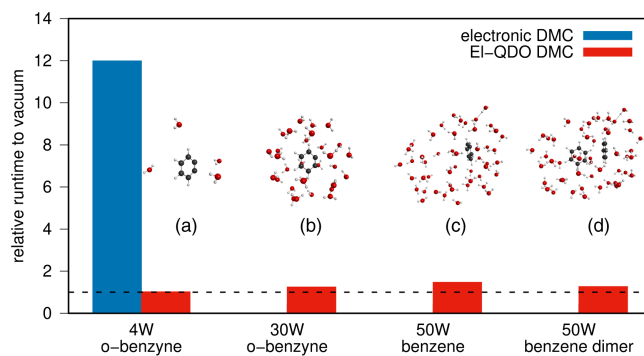

FIG. 4. Relative runtimes (see Supplemental Material [84]) of water-embedded El-QDO DMC calculations with respect to the molecular energies computed with DMC in vacuum. Runtime of electronic DMC is also shown for orthobenzyne in 4 W cage. Inset figures (a) to (d) correspond to the molecular structures [120,121].

TABLE I. Solvation energies (in kcal/mol) of the T-shaped benzene dimer and its monomers in the 50 W water cage [121] [Molecular structures (c) and (d) in Fig. 4].

	PBE0[a]	PBE0[a] + TS	PBE0[a] + MBD	DMC[b] El-FF	DMC[b] El-QDO
Monomer$_1$	−1.5	−4.1	−3.8	−3.48(6)	−4.0(1)
Monomer$_2$	−3.4	−6.6	−6.1	−5.18(6)	−6.4(1)
Dimer	−4.9	−10.9	−10.0	−8.9(1)	−10.3(2)

[a]PBE0 calculations are all-electrons (see Supplemental Material [84] for further details).
[b]DMC calculations are done using pseudopotentials discussed in [84].

with state-of-the-art DFT calculations using the PBE0 functional [122] augmented with the Tkatchenko-Scheffler pairwise dispersion energy (PBE0 + TS) [74] or the many-body dispersion method (PBE0 + MBD) [67,84,111] and with QM/MM DMC using the TIP3P water model [123] with pairwise vdW potentials [124] (El-FF).

From the results reported in Tables I and II we conclude that El-QDO DMC solvation energies are in excellent agreement with fully electronic DMC calculations (for the 4W cage for which they are feasible) and with PBE0 + MBD results. It is known that PBE0 + MBD binding energies are often quantitatively accurate for molecular systems, especially when compared to electronic DMC calculations [53]. In fact, we note that many-body effects are particularly evident for orthobenzyne, where the PBE0 + TS method overestimates the energies when compared to the El-QDO DMC and PBE0 + MBD methods, which both include, in a different manner, the many-body correlation effects of the environment on the solute. El-FF DMC yields quantitatively correct solvation energies for the smallest water cages, but for the larger environment, where the pairwise vdW part represents up to 70% of the total interaction energy (see Supplemental Material [84]), the error increases to 1 kcal/mol.

Another successful application of our El-QDO DMC approach can be observed in the singlet-triplet (S-T) adiabatic excitation energy of orthobenzyne (Table III). Because of delocalization error, DFT severely underestimates the S-T gap [120], while electronic DMC yields accurate results [125] in vacuum in excellent agreement

with the experimental value of 37.5(3) kcal/mol [126]. For the smallest cage of four water molecules, the excitation energies computed with electronic DMC and the El-QDO DMC approach are in excellent agreement with each other. Yet, the error bar of El-QDO calculations is much lower compared to electronic DMC computations for an equivalent sampling length. Moreover, as Table III shows, when increasing the size of the water cage, the excitation energy changes by 0.2(1) kcal/mol. This effect, captured by the El-QDO DMC, and consistent with other methods, arises from the higher polarization of the T state with respect to the S state of orthobenzyne. Interestingly, the El-FF approach predicts the same S-T gaps in the water cages, as the El-QDO approach, due to the correct description of the polarization effects at those distances and the very small changes of the vdW contributions between the two states, leading to nearly perfect error cancellation (see Supplemental Material [84]). We expect that future extensions of our method will allow more realistic embedding geometries where water molecules can come closer to the solute, yielding more substantial solvation effects. Remarkably, the computational cost of the El-QDO method is essentially independent of the number of QDOs in the embedding region (see Fig. 4) with respect to the cost of the molecule in vacuum. For the 4-water cage, the cost increases by only ∼2%, and by ∼25% for the 30-water cage. This stems from the lack of nodal structure in the QDO wave functions and low noise in their DMC sampling with respect to the electronic wave functions.

Our study illustrates the need for fully quantum embedding methods when treating binding and excitation energies

TABLE II. Solvation energies (in kcal/mol) of orthobenzyne [120] in its singlet and triplet spin states in cages of four (4 W) and thirty (30 W) water molecules [Molecular structures (a) and (b) in Fig. 4].

	PBE0[a]	PBE0[a] +TS	PBE0[a] +MBD	DMC[b]	DMC[b] El-FF	DMC[b] El-QDO
S (4W)	−1.01	−1.50	−1.43	−1.5(1)	−1.30(5)	−1.39(5)
T (4W)	−0.77	−1.24	−1.18	−1.0(1)	−1.11(5)	−1.12(5)
S (30W)	−2.82	−6.78	−6.11	⋯	−5.44(5)	−6.20(7)
T (30W)	−2.37	−6.41	−5.71	⋯	−4.99(5)	−5.73(7)

[a]PBE0 calculations are all-electrons (see Supplemental Material [84] for further details).
[b]DMC calculations are done using pseudopotentials discussed in [84].

TABLE III. Singlet-triplet adiabatic excitation energies of the orthobenzyne [120] in vacuum (V), 4-water cage (4 W), and 30-water cage (30 W) (in kcal/mol), corresponding to the molecular structures (a) and (b) in Fig. 4. The experimental value from ultraviolet photoelectron spectroscopy is estimated to be 37.5(3) [126].

	PBE0[a]	PBE0[a] + TS	PBE0[a] + MBD	DMC[b,c]	DMC[b,c] El-FF	DMC[b,c] El-QDO
S-T (V)	28.23	28.23	28.26	37.23(5)	⋯	⋯
S-T (4W)	28.46	28.48	28.51	37.7(1)	37.43(5)	37.50(5)
S-T (30W)	28.68	28.61	28.66	⋯	37.68(5)	37.70(8)

[a]PBE0 calculations are all-electrons (see Supplemental Material [84] for further details).
[b]DMC calculations are done using pseudopotentials discussed in [84].
[c]The excitation energies are corrected with respect to the pseudopotential error discussed in [84].

of solvated systems, and introduces a computationally efficient approach. The El-QDO embedding method is a firm first step in this direction as we demonstrated in the example of prototypical dispersion and hydrogen-bonded dimers and for the solvation of benzene derivates. A future challenge includes the incorporation of a more general representation of the QDO environment and exchange effects, which could be achieved through a synergy with machine-learning methods [127–130].

[*]matej.ditte@uni.lu
[†]matteo.barborini@gmail.com
[‡]Corresponding author: alexandre.tkatchenko@uni.lu

[1] Q. Sun and G. K.-L. Chan, Acc. Chem. Res. **49**, 2705 (2016).
[2] L. O. Jones, M. A. Mosquera, G. C. Schatz, and M. A. Ratner, J. Am. Chem. Soc. **142**, 3281 (2020).
[3] J. Hermann, R. A. DiStasio, and A. Tkatchenko, Chem. Rev. **117**, 4714 (2017).
[4] A. R. Fersht, Proc. Natl. Acad. Sci. U.S.A. **110**, 19656 (2013).
[5] R. Khare, S. L. Mielke, J. T. Paci, S. Zhang, R. Ballarini, G. C. Schatz, and T. Belytschko, Phys. Rev. B **75**, 075412 (2007).
[6] J. Torras, F. Rodríguez-Ropero, O. Bertran, and C. Alemán, J. Phys. Chem. C **113**, 3574 (2009).
[7] P. M. Zimmerman, M. Head-Gordon, and A. T. Bell, J. Chem. Theory Comput. **7**, 1695 (2011).
[8] V. A. Nasluzov, V. V. Rivanenkov, A. B. Gordienko, K. M. Neyman, U. Birkenheuer, and N. Rösch, J. Chem. Phys. **115**, 8157 (2001).
[9] V. A. Nasluzov, E. A. Ivanova, A. M. Shor, G. N. Vayssilov, U. Birkenheuer, and N. Rösch, J. Phys. Chem. B **107**, 2228 (2003).
[10] M. Brändle and J. Sauer, J. Am. Chem. Soc. **120**, 1556 (1998).
[11] R. Guareschi, H. Zulfikri, C. Daday, F. M. Floris, C. Amovilli, B. Mennucci, and C. Filippi, J. Chem. Theory Comput. **12**, 1674 (2016).
[12] H. M. Senn and W. Thiel, Angew. Chem., Int. Ed. Engl. **48**, 1198 (2009).
[13] O. Acevedo and W. L. Jorgensen, Acc. Chem. Res. **43**, 142 (2010).
[14] M. Huang, T. Dissanayake, E. Kuechler, B. K. Radak, T.-S. Lee, T. J. Giese, and D. M. York, J. Chem. Theory Comput. **13**, 3975 (2017).
[15] C. N. Alves, J. R. A. Silva, and A. E. Roitberg, Phys. Chem. Chem. Phys. **17**, 17790 (2015).
[16] J. R. A. Silva, A. E. Roitberg, and C. N. Alves, J. Phys. Chem. B **119**, 1468 (2015).
[17] L. Bao, W. Liu, Y. Li, X. Wang, F. Xu, Z. Yang, Y. Yue, C. Zuo, Q. Zhang, and W. Wang, Chem. Res. Toxicol. **32**, 603 (2019).
[18] M. d. C. Marín, L. De Vico, S. S. Dong, L. Gagliardi, D. G. Truhlar, and M. Olivucci, J. Chem. Theory Comput. **15**, 1915 (2019).
[19] A. Robertazzi and J. A. Platts, J. Phys. Chem. A **110**, 3992 (2006).
[20] K. Gkionis and J. Platts, J. Biol. Inorg. Chem. **14**, 1165 (2009).
[21] S. Kupfer, L. Zedler, J. Guthmuller, S. Bode, M. D. Hager, U. S. Schubert, J. Popp, S. Gräfe, and B. Dietzek, Phys. Chem. Chem. Phys. **16**, 12422 (2014).
[22] S. Osoegawa, R. Miyoshi, K. Watanabe, Y. Hirose, T. Fujisawa, M. Ikeuchi, and M. Unno, J. Phys. Chem. B **123**, 3242 (2019).
[23] D. Loco and J.-P. Piquemal, in *Photochemistry: Volume 50* (The Royal Society of Chemistry, 2022), pp. 386–402.
[24] H. M. Cho and W. A. Lester, Jr., J. Phys. Chem. Lett. **1**, 3376 (2010).
[25] G. Kotliar, S. Y. Savrasov, K. Haule, V. S. Oudovenko, O. Parcollet, and C. A. Marianetti, Rev. Mod. Phys. **78**, 865 (2006).
[26] T. N. Lan, A. A. Kananenka, and D. Zgid, J. Chem. Phys. **143**, 241102 (2015).

[27] G. Knizia and G. K.-L. Chan, Phys. Rev. Lett. **109,** 186404 (2012).

[28] T. A. Wesolowski, S. Shedge, and X. Zhou, Chem. Rev. **115,** 5891 (2015).

[29] F. Libisch, C. Huang, and E. A. Carter, Acc. Chem. Res. **47,** 2768 (2014).

[30] F. R. Manby, M. Stella, J. D. Goodpaster, and T. F. Miller, III, J. Chem. Theory Comput. **8,** 2564 (2012).

[31] K. P. Katin, V. S. Prudkovskiy, and M. M. Maslov, Phys. Lett. A **381,** 2686 (2017).

[32] J. Friedrich, M. Hanrath, and M. Dolg, J. Chem. Phys. **126,** 154110 (2007).

[33] M. Seth, P. M. Margl, and T. Ziegler, Macromolecules **35,** 7815 (2002).

[34] K. D. Vogiatzis, W. Klopper, and J. Friedrich, J. Chem. Theory Comput. **11,** 1574 (2015).

[35] P. Huo, C. Uyeda, J. D. Goodpaster, J. C. Peters, and T. F. Miller, III, ACS Catal. **6,** 6114 (2016).

[36] S. J. R. Lee, M. Welborn, F. R. Manby, and T. F. Miller, III, Acc. Chem. Res. **52,** 1359 (2019).

[37] D. J. Coughtrie, R. Giereth, D. Kats, H.-J. Werner, and A. Köhn, J. Chem. Theory Comput. **14,** 693 (2018).

[38] J. Neugebauer, M. J. Louwerse, E. J. Baerends, and T. A. Wesolowski, J. Chem. Phys. **122,** 094115 (2005).

[39] C. R. Jacob and L. Visscher, J. Chem. Phys. **125,** 194104 (2006).

[40] T. E. Exner, A. Frank, I. Onila, and H. M. Möller, J. Chem. Theory Comput. **8,** 4818 (2012).

[41] T. E. Exner and P. G. Mezey, J. Phys. Chem. A **108,** 4301 (2004).

[42] M. Bockstedte, F. Schütz, T. Garratt, V. Ivády, and A. Gali, npj Quantum Mater. **3,** 31 (2018).

[43] B. T. G. Lau, G. Knizia, and T. C. Berkelbach, J. Phys. Chem. Lett. **12,** 1104 (2021).

[44] T. Schäfer, A. Gallo, A. Irmler, F. Hummel, and A. Grüneis, J. Chem. Phys. **155,** 244103 (2021).

[45] H. Ma, N. Sheng, M. Govoni, and G. Galli, J. Chem. Theory Comput. **17,** 2116 (2021).

[46] F. Petocchi, F. Nilsson, F. Aryasetiawan, and P. Werner, Phys. Rev. Res. **2,** 013191 (2020).

[47] C.-N. Yeh, S. Iskakov, D. Zgid, and E. Gull, Phys. Rev. B **103,** 195149 (2021).

[48] E. A. Nowadnick, J. P. Ruf, H. Park, P. D. C. King, D. G. Schlom, K. M. Shen, and A. J. Millis, Phys. Rev. B **92,** 245109 (2015).

[49] H. Chen, A. Hampel, J. Karp, F. Lechermann, and A. J. Millis, Front. Phys. **10,** 835942 (2022).

[50] M. Nusspickel and G. H. Booth, Phys. Rev. X **12,** 011046 (2022).

[51] D. Bovi, D. Narzi, and L. Guidoni, Angew. Chem., Int. Ed. Engl. **52,** 11744 (2013).

[52] A. Benali, L. Shulenburger, N. A. Romero, J. Kim, and O. A. von Lilienfeld, J. Chem. Theory Comput. **10,** 3417 (2014).

[53] Y. S. Al-Hamdani, P. R. Nagy, A. Zen, D. Barton, M. Kállay, J. G. Brandenburg, and A. Tkatchenko, Nat. Commun. **12,** 3927 (2021).

[54] D. Reta Mañeru, A. K. Pal, I. d. P. R. Moreira, S. N. Datta, and F. Illas, J. Chem. Theory Comput. **10,** 335 (2014).

[55] J.-N. Boyn and D. A. Mazziotti, J. Chem. Phys. **154,** 134103 (2021).

[56] J. L. Bao, A. Sand, L. Gagliardi, and D. G. Truhlar, J. Chem. Theory Comput. **12,** 4274 (2016).

[57] D. Varsano, S. Sorella, D. Sangalli, M. Barborini, S. Corni, E. Molinari, and M. Rontani, Nat. Commun. **8,** 1461 (2017).

[58] M. Barborini, M. Calandra, F. Mauri, L. Wirtz, and P. Cudazzo, Phys. Rev. B **105,** 075122 (2022).

[59] Z. D. Pozun, X. Su, and K. D. Jordan, J. Am. Chem. Soc. **135,** 13862 (2013).

[60] M. Barborini and E. Coccia, J. Chem. Theory Comput. **11,** 5696 (2015).

[61] M. Abe, Chem. Rev. **113,** 7011 (2013).

[62] R. J. Bartlett and M. Musiał, Rev. Mod. Phys. **79,** 291 (2007).

[63] W. M. C. Foulkes, L. Mitas, R. J. Needs, and G. Rajagopal, Rev. Mod. Phys. **73,** 33 (2001).

[64] M. H. Kalos and P. A. Whitlock, Quantum Monte Carlo, in *Monte Carlo Methods* (John Wiley & Sons, Ltd, New York, 2008), Chap. 8, pp. 159–178.

[65] F. Becca and S. Sorella, *Quantum Monte Carlo Approaches for Correlated Systems* (Cambridge University Press, Cambridge, England, 2017).

[66] A. Jones, A. Thompson, J. Crain, M. H. Müser, and G. J. Martyna, Phys. Rev. B **79,** 144119 (2009).

[67] A. Tkatchenko, R. A. DiStasio, R. Car, and M. Scheffler, Phys. Rev. Lett. **108,** 236402 (2012).

[68] A. Jones, F. Cipcigan, V. P. Sokhan, J. Crain, and G. J. Martyna, Phys. Rev. Lett. **110,** 227801 (2013).

[69] A. Jones, J. Crain, F. Cipcigan, V. Sokhan, M. Modani, and G. Martyna, Mol. Phys. **111,** 3465 (2013).

[70] A. P. Jones, J. Crain, V. P. Sokhan, T. W. Whitfield, and G. J. Martyna, Phys. Rev. B **87,** 144103 (2013).

[71] T. Odbadrakh, V. Voora, and K. Jordan, Chem. Phys. Lett. **630,** 76 (2015).

[72] T. T. Odbadrakh and K. D. Jordan, J. Chem. Phys. **144,** 034111 (2016).

[73] F. S. Cipcigan, J. Crain, V. P. Sokhan, and G. J. Martyna, Rev. Mod. Phys. **91,** 025003 (2019).

[74] A. Tkatchenko and M. Scheffler, Phys. Rev. Lett. **102,** 073005 (2009).

[75] O. Vaccarelli, D. V. Fedorov, M. Stöhr, and A. Tkatchenko, Phys. Rev. Res. **3,** 033181 (2021).

[76] P. P. Poier, L. Lagardère, and J.-P. Piquemal, J. Chem. Theory Comput. **18,** 1633 (2022).

[77] M. R. Karimpour, D. V. Fedorov, and A. Tkatchenko, Phys. Rev. Res. **4,** 013011 (2022).

[78] M. R. Karimpour, D. V. Fedorov, and A. Tkatchenko, J. Phys. Chem. Lett. **13,** 2197 (2022).

[79] J. A. Lemkul, J. Huang, B. Roux, and A. D. MacKerell, Jr., Chem. Rev. **116,** 4983 (2016).

[80] A. T. Bui, F. L. Thiemann, A. Michaelides, and S. J. Cox, Nano Lett. **23,** 580 (2023).

[81] T. Sommerfeld and K. D. Jordan, J. Phys. Chem. A **109,** 11531 (2005).

[82] D. J. Margoliash and W. J. Meath, J. Chem. Phys. **68,** 1426 (1978).

[83] S. Góger, A. Khabibrakhmanov, O. Vaccarelli, D. V. Fedorov, and A. Tkatchenko, J. Phys. Chem. Lett. **14,** 6217 (2023).

[84] See Supplemental Material at http://link.aps.org/supplemental/10.1103/PhysRevLett.131.228001 for further

details on the drudon-electron model, the quantum Monte Carlo methods, the computational details of the calculations, and the construction and geometries of the water cages [85–105].

[85] N. Metropolis, A. W. Rosenbluth, M. N. Rosenbluth, A. H. Teller, and E. Teller, J. Chem. Phys. **21,** 1087 (1953).

[86] W. K. Hastings, Biometrika **57,** 97 (1970).

[87] C. Filippi and C. J. Umrigar, Phys. Rev. B **61,** R16291 (2000).

[88] M. Casula, C. Attaccalite, and S. Sorella, J. Chem. Phys. **121,** 7110 (2004).

[89] M. Marchi, S. Azadi, C. Casula, and S. Sorella, J. Chem. Phys. **131,** 154116 (2009).

[90] F. Sterpone, L. Spanu, L. Ferraro, S. Sorella, and L. Guidoni, J. Chem. Theory Comput. **4,** 1428 (2008).

[91] I. Kosztin, B. Faber, and K. Schulten, Am. J. Phys. **64,** 633 (1996).

[92] L. Mitas, in Quantum Monte Carlo Methods in Physics and Chemistry, NATO ASI Series, Series C, Math. & Phys. Sciences Vol. C-525, edited by M. P. Nightingale and C. J. Umrigar (Kluwer Academic Publishers, Boston, 1999).

[93] C. J. Umrigar, M. P. Nightingale, and K. J. Runge, J. Chem. Phys. **99,** 2865 (1993).

[94] G. Wang, A. Annaberdiyev, C. A. Melton, M. C. Bennett, L. Shulenburger, and L. Mitas, J. Chem. Phys. **151,** 144110 (2019).

[95] M. C. Bennett, G. Wang, A. Annaberdiyev, C. A. Melton, L. Shulenburger, and L. Mitas, J. Chem. Phys. **149,** 104108 (2018).

[96] A. Annaberdiyev, G. Wang, C. A. Melton, M. C. Bennett, L. Shulenburger, and L. Mitas, J. Chem. Phys. **149,** 134108 (2018).

[97] M. C. Bennett, C. A. Melton, A. Annaberdiyev, G. Wang, L. Shulenburger, and L. Mitas, J. Chem. Phys. **147,** 224106 (2017).

[98] A. Zen, J. G. Brandenburg, A. Michaelides, and D. Alfè, J. Chem. Phys. **151,** 134105 (2019).

[99] A. Zen, S. Sorella, M. J. Gillan, A. Michaelides, and D. Alfè, Phys. Rev. B **93,** 241118(R) (2016).

[100] G. M. J. Barca et al., J. Chem. Phys. **152,** 154102 (2020).

[101] F. Neese, F. Wennmohs, U. Becker, and C. Riplinger, J. Chem. Phys. **152,** 224108 (2020).

[102] V. Blum, R. Gehrke, F. Hanke, P. Havu, V. Havu, X. Ren, K. Reuter, and M. Scheffler, Comput. Phys. Commun. **180,** 2175 (2009).

[103] P. K. Biswas and V. Gogonea, J. Chem. Phys. **123,** 164114 (2005).

[104] J. M. Waldrop, B. Song, K. Patkowski, and X. Wang, J. Chem. Phys. **142,** 204307 (2015).

[105] R. Hellmann, B. Jäger, and E. Bich, J. Chem. Phys. **147,** 034304 (2017).

[106] M. Sadhukhan and F. R. Manby, Phys. Rev. B **94,** 115106 (2016).

[107] B. M. Austin, D. Y. Zubarev, and W. A. Lester, Jr., Chem. Rev. **112,** 263 (2012).

[108] M. Barborini, Quantum Mecha (QMeCha) package (private repository March 2023).

[109] S. Sorella, Phys. Rev. B **64,** 024512 (2001).

[110] S. Sorella, Phys. Rev. B **71,** 241103(R) (2005).

[111] A. Ambrosetti, A. M. Reilly, R. A. DiStasio, and A. Tkatchenko, J. Chem. Phys. **140,** 18A508 (2014).

[112] M. Dubecký, L. Mitas, and P. Jurečka, Chem. Rev. **116,** 5188 (2016).

[113] K. Patkowski, G. Murdachaew, C.-M. Fou, and K. Szalewicz, Mol. Phys. **103,** 2031 (2005).

[114] M. P. Metz, K. Szalewicz, J. Sarka, R. Tóbiás, A. G. Császár, and E. Mátyus, Phys. Chem. Chem. Phys. **21,** 13504 (2019).

[115] D. V. Fedorov, M. Sadhukhan, M. Stöhr, and A. Tkatchenko, Phys. Rev. Lett. **121,** 183401 (2018).

[116] L. Shirkov and V. Sladek, J. Chem. Phys. **147,** 174103 (2017).

[117] A. Altun, F. Neese, and G. Bistoni, Beilstein J. Org. Chem. **14,** 919 (2018).

[118] R. A. DiStasio, G. von Helden, R. P. Steele, and M. Head-Gordon, Chem. Phys. Lett. **437,** 277 (2007).

[119] K. Carter-Fenk and J. M. Herbert, Chem. Sci. **11,** 6758 (2020).

[120] J. Shee, E. J. Arthur, S. Zhang, D. R. Reichman, and R. A. Friesner, J. Chem. Theory Comput. **15,** 4924 (2019).

[121] D. A. Sirianni, X. Zhu, D. F. Sitkoff, D. L. Cheney, and C. D. Sherrill, J. Chem. Phys. **156,** 194306 (2022).

[122] C. Adamo and V. Barone, J. Chem. Phys. **110,** 6158 (1999).

[123] W. L. Jorgensen, J. Chandrasekhar, J. D. Madura, R. W. Impey, and M. L. Klein, J. Chem. Phys. **79,** 926 (1983).

[124] W. L. Jorgensen and D. L. Severance, J. Am. Chem. Soc. **112,** 4768 (1990).

[125] X. Zhou and F. Wang, Phys. Chem. Chem. Phys. **21,** 20422 (2019).

[126] P. G. Wenthold, R. R. Squires, and W. C. Lineberger, J. Am. Chem. Soc. **120,** 5279 (1998).

[127] O. T. Unke, S. Chmiela, H. E. Sauceda, M. Gastegger, I. Poltavsky, K. T. Schütt, A. Tkatchenko, and K.-R. Müller, Chem. Rev. **121,** 10142 (2021).

[128] M. Stöhr, L. Medrano Sandonas, and A. Tkatchenko, J. Phys. Chem. Lett. **11,** 6835 (2020).

[129] O. Unke, S. Chmiela, M. Gastegger, K. Schütt, H. E. Sauceda, and K.-R. Müller, Nat. Commun. **12,** 7273 (2021).

[130] J. Hermann, Z. Schätzle, and F. Noé, Nat. Chem. **12,** 891 (2020).

[131] S. Varrette, P. Bouvry, H. Cartiaux, and F. Georgatos, in Proceedings of the 2014 International Conference on High Performance Computing & Simulation (HPCS 2014) (IEEE, Bologna, Italy, 2014), pp. 959–967.